ADVANCED MATERIALS

[9] V. Georgakilas, K. Kordatos, M. Prato, D. M. Guldi, M. Holzinger, A. Hirsch, *J. Am. Chem. Soc.* **2002**, *124*, 760.

[10] D. M. Guldi, M. Marcaccio, D. Paolucci, F. Paolucci, N. Tagmatarchis, D. Tasis, E. Vázquez, M. Prato, *Angew. Chem. Int. Ed.* **2003**, *42*, 4206.

[11] H. Murakami, T. Nomura, N. Nakashima, *Chem. Phys. Lett.* **2003**, *378*, 481.

[12] a) U. Resch, M. A. Fox, *J. Phys. Chem.* **1991**, *95*, 6169. b) U. Resch, M. A. Fox, *J. Phys. Chem.* **1991**, *95*, 6316. c) N. Kanayama, T. Kanbara, H. Kitano, *J. Phys. Chem. B* **2000**, *104*, 271. d) H. Imahori, H. Norieda, Y. Nishimura, I. Yamazaki, K. Higuchi, N. Kato, T. Motohiro, H. Yamada, K. Tamaki, M. Arimura, Y. Sakata, *J. Phys. Chem. B* **2000**, *104*, 1253.

[13] a) M. Lahav, V. Heleg-Shabtai, J. Wasserman, E. Katz, I. Willner, H. Dürr, Y.-Z. Hu, S. H. Bossmann, *J. Am. Chem. Soc.* **2000**, *122*, 11480. b) F. B. Abdelrazzaq, R. C. Kwong, M. E. Thompson, *J. Am. Chem. Soc.* **2002**, *124*, 4796.

[14] D. M. Guldi, M. Prato, *Acc. Chem. Res.* **2000**, *33*, 695.

[15] a) H. Imahori, H. Yamada, D. M. Guldi, Y. Endo, A. Shimomura, S. Kundu, K. Yamada, T. Okada, Y. Sakata, S. Fukuzumi, *Angew. Chem. Int. Ed.* **2002**, *41*, 2344. b) H. Yamada, H. Imahori, Y. Nishimura, I. Yamazaki, T. K. Ahn, S. K. Kim, D. Kim, S. Fukuzumi, *J. Am. Chem. Soc.* **2003**, *125*, 9129.

[16] Y.-P. Sun, W. J. Huang, Y. Lin, K. F. Fu, A. Kitaygorodskiy, L. A. Riddle, Y. J. Yu, D. L. Carroll, *Chem. Mater.* **2001**, *13*, 2864.

[17] a) J. Chen, M. A. Hamon, H. Hu, Y. Chen, A. M. Rao, P. C. Eklund, R. C. Haddon, *Science* **1998**, *282*, 95. b) M. A. Hamon, M. E. Itkis, S. Niyogi, T. Alvaraez, C. Kuper, M. Menon, R. C. Haddon, *J. Am. Chem. Soc.* **2001**, *123*, 11 292.

[18] a) J. Zhu, J. Kim, H. Peng, J. L. Margrave, V. N. Khabashesku, E. V. Barrera, *Nano Lett.* **2003**, *3*, 1107. b) S. Qin, D. Qin, W. T. Ford, D. E. Resasco, J. E. Herrera, *J. Am. Chem. Soc.* **2004**, *126*, 170.

[19] a) Y.-P. Sun, K. Fu, Y. Lin, W. Huang, *Acc. Chem. Res.* **2002**, *35*, 1096. b) J. E. Riggs, Z. X. Guo, D. L. Carroll, Y.-P. Sun, *J. Am. Chem. Soc.* **2000**, *122*, 5879. c) Y.-P. Sun, B. Zhou, K. Henbest, K. Fu, W. J. Huang, Y. Lin, S. Taylor, D. L. Carroll, *Chem. Phys. Lett.* **2002**, *351*, 349.

[20] Y. Lin, D. E. Hill, J. Bentley, J. F. Allard, Y.-P. Sun, *J. Phys. Chem. B* **2003**, *108*, 10 453.

[21] J. B. Birks, *Organic Molecular Photophysics*, Wiley, Chichester, UK **1970**.

[22] R. B. Martin, K. Fu, Y.-P. Sun, *Chem. Phys. Lett.* **2003**, *375*, 619.

[23] The observed fluorescence decays of **1** and **2** are monoexponential, with lifetimes of 9.1 ns and 9.2 ns, respectively. While appearing similar, the decays of **I** and **II** deviate slightly from the monoexponential function, probably due to some minor luminescence interference from the functionalized SWNTs [19].

[24] J. Liu, A. G. Rinzler, H. J. Dai, J. H. Hafner, R. K. Bradley, P. J. Boul, A. Lu, T. Iverson, K. Shelimov, C. B. Huffman, F. Rodriguez-Macias, Y. S. Shon, T. R. Lee, D. T. Colbert, R. E. Smalley, *Science* **1998**, *280*, 1253.

[25] W. Huang, S. Fernando, L. F. Allard, Y.-P. Sun, *Nano Lett.* **2003**, *3*, 565.

[26] a) E. M. Harth, S. Hecht, B. Helms, E. E. Malmstrom, J. M. J. Frechet, C. J. Hawker, *J. Am. Chem. Soc.* **2002**, *124*, 3926. b) H. K. Hombrecher, S. Ohm, *Tetrahedron* **1993**, *49*, 2447.

Si-Compatible Ion Selective Oxide Interconnects with High Tunability**

By *Riaan Schmuhl*, *Jelena Sekulic*, *Sankhanilay Roy Chowdhury*, *Cees J. M. van Rijn*, *Klaas Keizer*, *Albert van den Berg*, *Johan E. ten Elshof*,* and *Dave H. A. Blank*

Switchable interconnects for controlled transport of molecular or ionic species, charged nanoparticles, or biomolecules may lead to microchip-based technologies for molecular separation, detection, and dosing. One of the issues in microfluidic device technology concerns the development of such selective gates. Although permselective mesoporous and microporous oxide membranes with well-defined pore sizes and pore architectures on ceramic supports have been developed in the past years, their application in microfluidic devices remains a challenge due to the need for these films to be compatible with silicon technology. The current interest in microfluidics is largely motivated by their envisaged applications. Microfluidic analyses are quickly becoming an established technology in analytical chemistry and biotechnology,[1] while the large potential that microfluidic approaches may offer in the field of synthetic chemistry has only just started to be explored.[2] Microchip-based fluidic devices for chemical analyses or syntheses have several unique advantages over macroscopic approaches, such as a very high degree of temporal control over temperature and chemical environment, high accuracy, and relatively easy automation and integration of functional components like heaters, temperature controllers, and feeding channels.[3,4] To date, selective interconnects for microfluidic devices[4,5] have been based on track-etched polymeric (NTEP) membranes and anodic aluminum oxide (AAO) thin films.[6] For instance, Sweedler, Bohn, and co-workers[7] developed a gateable interconnect for analyte injection in microfluidic devices based on an NTEP membrane. Martin et al. showed how to influence the ion permselectivity of gold-plated NTEP membranes by imposing a bias potential on the membrane.[8] NTEP membranes are made by bombarding 6–20 μm thick nonporous sheets of polycarbonate or polyester with nuclear fission fragments. This creates straight dam-

[*] Dr. J. E. ten Elshof, R. Schmuhl, J. Sekulic, S. Roy Chowdhury, Dr. K. Keizer, Prof. D. H. A. Blank
Inorganic Materials Science, Faculty of Science and Technology
MESA+ Institute for Nanotechnology, University of Twente
PO Box 217, 7500 AE, Enschede (The Netherlands)
E-mail: j.e.tenelshof@utwente.nl

Dr. C. J. M. van Rijn
Aquamarijn Micro Filtration B.V.
Beatrixlaan 2, 7255 DB, Hengelo Gld. (The Netherlands)

Prof. A. van den Berg
Laboratory of Biosensors, Faculty of Electrical Engineering
MESA+ Institute for Nanotechnology, University of Twente
PO Box 217, 7500 AE, Enschede (The Netherlands)

[**] Part of this work was financially supported by the Netherlands Technology Foundation (STW).

  DOI: 10.1002/adma.200306660

age tracks in the sheet, which are subsequently turned into pores using chemical etching. Commercially available NTEP membranes have pores densities of $3–10 \times 10^8$ cm^{-2} and pore diameters down to 10–15 nm.[7] AAO films are thicker, typically ~50 μm, and contain straight cylindrical pores of 20 nm diameter or larger. They are prepared by anodization of aluminum metal foils in acidic solutions and have porosities of 25–40 %, much higher than in NTEP membranes.

The oxide interconnects were made of mesoporous γ-alumina or silica, and microporous titania.[8–11] These oxide layers are less than 1 μm thick, have a total porosity of 35–60 %, and pore diameters in the range of only 0.8–8 nm (see Table 1). Unlike NTEP and AAO membranes they do not have a straight channel pores, but have a disordered or mesostructured template-directed pore structure. To give these layers sufficient mechanical stability they are deposited onto 0.5 cm × 0.5 cm Si-based microsieves of 1 μm effective thickness, which contain areas with hexagonal arrays of circular perforations of 0.5 or 1.2 μm.[12] The overall porosity of the sieves is 30 %.

A scanning electron microscope (SEM) picture indicating the pattern of perforated areas is shown in Figure 1a, and a close-up of a perforated area is shown in Figure 1b. Interconnects with different types of oxide top layers were prepared, namely conventional mesoporous γ-alumina layers, mesoporous MCM-48 silica layers obtained by template-directed synthesis of self-assembled surfactants,[11] and microporous amorphous titania layers. Figure 1c shows an interconnect with a calcined MCM-48 layer that was deposited on the microsieve by spin-coating. The MCM-48 layer penetrates the perforations of the sieve and is about 970 nm thick in the center of the perforations. The thicknesses of the different oxide films are indicated in Table 1. The thickness varied depending on the concentrations of the sols, and variations in diameter of the 0.5–1.2 μm perforations. A top view of a microsieve covered by spin-coating with γ-alumina is shown in Figure 1d.

The presence of ordered mesoporosity in the silica films is illustrated in Figure 2a, where a small-angle X-ray diffraction (XRD) pattern of a calcined silica film spin-coated on a silicon substrate is shown. The pattern matches that of an ordered mesoporous MCM-48 phase with unit cell $a \approx 9.4$ nm.[13] The peak at 2θ 2.3° and the shoulder at 2.6° are the 211 and 220 reflections, respectively, while the broad shallow peak at 2θ 4.5–6° indicates a series of higher-order reflections. The average pore diameter of MCM-48 was determined by nitrogen sorption on unsupported MCM-48 powder and was found to be 2.8–3.4 nm. The distribution of Kelvin radii r_K in a supported γ-alumina thin film was determined by the permporometry technique[10] and is shown in Figure 2b. Since the pore diameter is equal to $2(r_K+t)$, where t is the t-layer thickness ($t = 0.3–0.4$ nm),[14] the pore sizes of γ-alumina are in the range of ~5–7.5 nm. Figure 2c shows the temperature-programmed XRD spectra of dried polymeric TiO_2 sols. The material retained its amorphous structure until 300–350 °C. At 400 °C a (partial) phase transformation into the crystalline anatase phase occurred. Unlike anatase, which is mesoporous, the amorphous phase of titania is microporous, and molecular weight cut-off nanofiltration experiments with poly(ethylene glycol) (PEG) solutions indicated that the pore size is < 0.8 nm.[15] The main physical and structural properties of the oxide top layers of which interconnects were made are summarized in Table 1. From the summary it is clear that

Table 1. Physical, structural, and transport properties oxide interconnects.

		TiO_2	MCM-48	γ-Al_2O_3
Iso-electric point		4.2–4.8	2–3	8.5–9
Pore size [nm]		~0.8 [a]	2.8–3.4 [b]	5–7.5 [c]
Porosity [%]		34–41 [d]	~60 [d]	~55 [b]
Film thickness [e] [nm]		~500	~970	~300
Permeability [cm^2 s^{-1}]	Fl^{2-}	$(3.5\pm0.8) \times 10^{-7}$	$(8.5\pm0.8) \times 10^{-8}$	$(3.9\pm0.2) \times 10^{-10}$ [f]
	MV^{2+}	$(3.1\pm0.3) \times 10^{-7}$	$(1.1\pm0.2) \times 10^{-6}$	$(5.9\pm0.4) \times 10^{-8}$
	d-Trp	$< 1.0 \times 10^{-11}$	$< 1.0 \times 10^{-11}$	$< 1.0 \times 10^{-11}$

[a] Based on molecular weight cut-off nanofiltration experiments with polyethylene glycol (PEG) solutions. [b] Based on nitrogen sorption data of unsupported calcined powder. [c] Determined by permporometry. [d] Estimated by reflectometry. [e] Thickness of the MCM-48 layer was determined on a microsieve with perforation of 1.2 μm, while for the others a microsieve with 500 nm perforations was used. [f] Transport experiments were done at pH 6.9, due to the lack of stability of the γ-alumina layer at > pH 8.

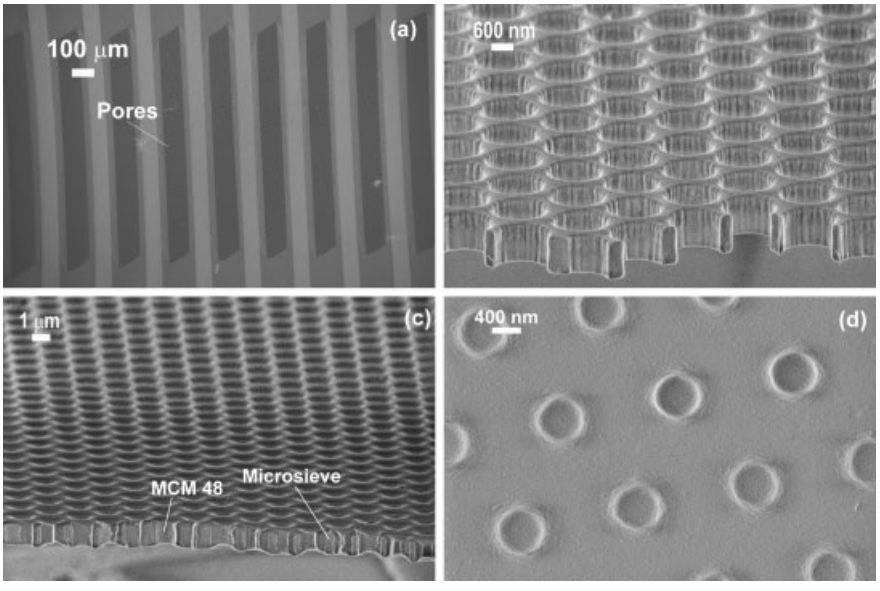

Figure 1. a) SEM picture of the perforation pattern on silicon nitride microsieves. b) Overview of uncoated 1.2 μm perforations. c) Cross-section of MCM-48 silica layer deposited on microsieve with 1.2 μm perforations. d) Top view of a spin-coated γ-alumina layer on a microsieve with 500 nm perforations.

ADVANCED MATERIALS

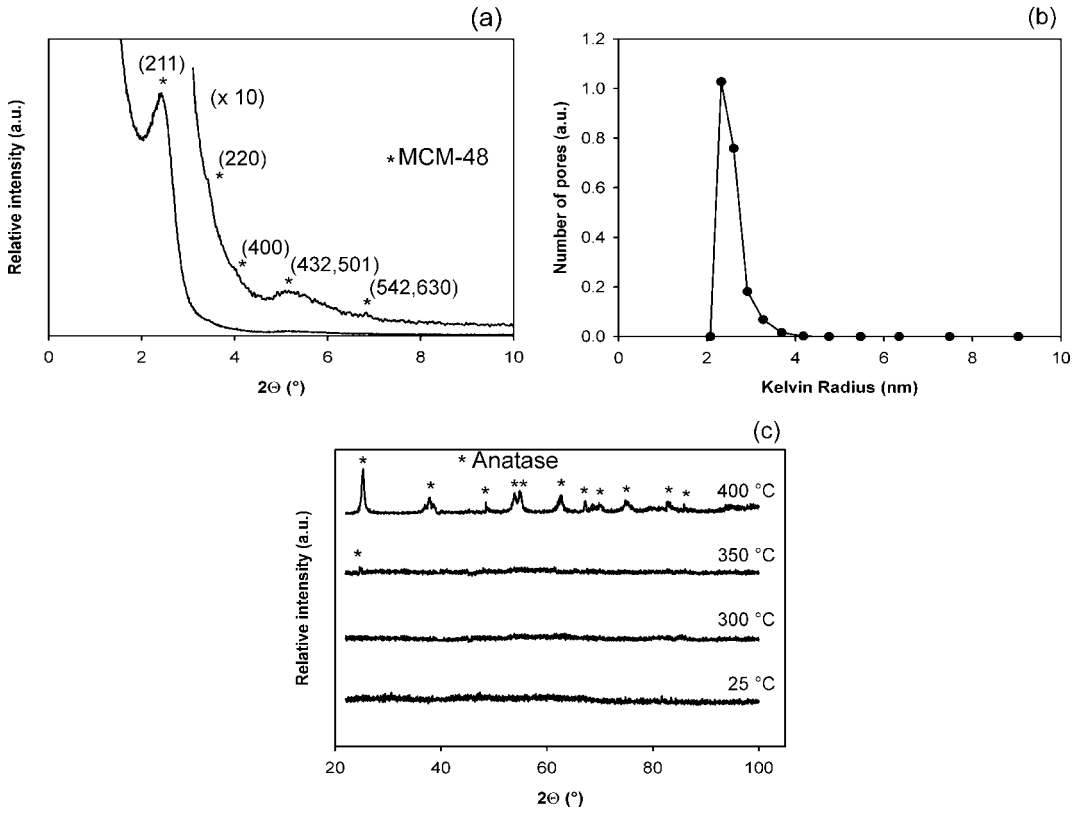

Figure 2. a) XRD diagrams of uncalcined air-dried and calcined MCM-48 silica thin films on silicon (004). b) Pore size distribution of γ-alumina film calcined at 600 °C as determined by permporometry. c) High-temperature XRD diagrams of amorphous microporous TiO_2.

oxide layers with different intrinsic materials properties can be fabricated.

Ion transport experiments were carried out with fluorescein (Fl^{2-}, Fluka), methylviologen (MV^{2+}, Aldrich) and d-tryptophan (d-Trp, Aldrich). The interconnects were placed between the two halves of a U-shaped tube. A direct current (DC) potential difference ΔV, defined as the potential at the receive (permeate) side relative to the potential at the feed side, was imposed over the interconnect using external Pt electrodes separated by 4 mm. The pH was maintained at 7.8–8.2 with a NaH_2PO_4/Na_2HPO_4 buffer solution. The interconnects were wetted in the buffer solution prior to the experiments.

Figure 3a shows the concentration increase of viologen (MV^{2+}) with time at the receive side after $\Delta V = -2$ V had been

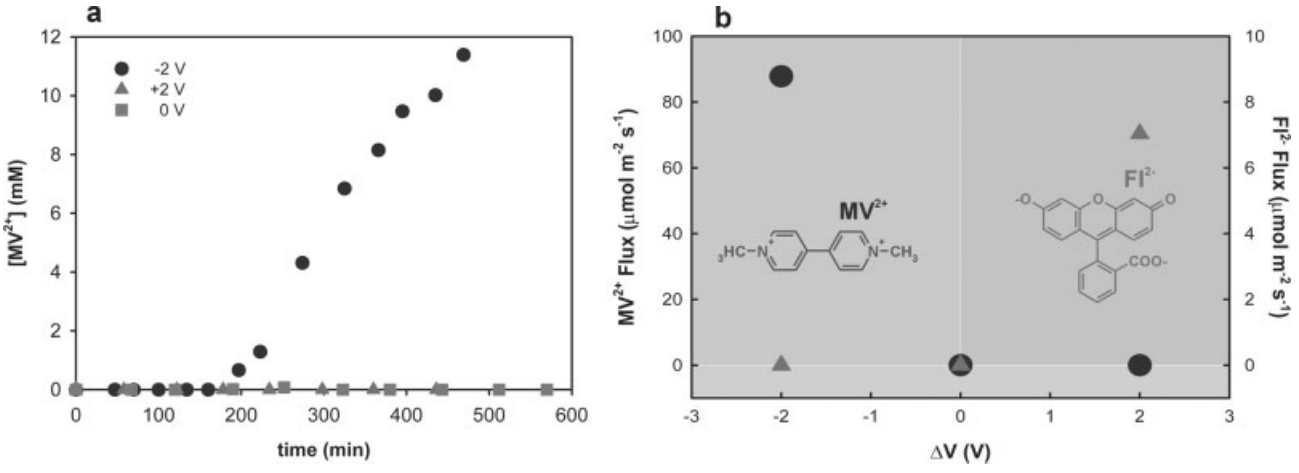

Figure 3. Transport phenomena of fluorescein (Fl^{2-}) and viologen (MV^{2+}) through a MCM-48 interconnect. a) Concentration increase of MV^{2+} at the receive side versus time at $\Delta V = -2$, 0 and +2 V. b) Fluxes of fluorescein (Fl^{2-}) and viologen (MV^{2+}) versus electrode potential difference ΔV. Feed-side probe concentration is 0.8 mM.

imposed. On the other hand no noticeable concentration increase occurred in 8 h time when $\Delta V \geq 0$. The opposite trend was observed for Fl^{2-}. In all experiments measurable ionic fluxes were directed towards an oppositely charged electrode at the receive side of the membrane. Any molecular and ionic flux resulting from electrical potential and/or concentration gradients is due to one or more of three mechanisms of transport: 1) Fick diffusion, which moves both charged and uncharged species under the influence of a concentration gradient, 2) electro-osmotic flow (EOF), which is driven by the mobile double-layer inside the pores and moves the entire liquid under the influence of an electric field gradient, and 3) ion migration, which moves charged species toward the oppositely charged electrode.[16] The absence of a noticeable flux of ionic species under field-off ($\Delta V = 0$) conditions indicates that transport by Fick diffusion is negligible, i.e., the gate is effectively closed. Experiments with uncharged d-Trp did not show significant fluxes within experimental error under either field-on or field-off conditions, which excludes solvent or ion transport by electro-osmotic flow. This strongly suggests that the interconnects transport species by ion migration. Hence, the behavior of the interconnects described here differs substantially from the NTEP nanofluidic gates with 15–200 nm channels developed by Sweedler, Bohn, and coworkers.[17] Transport through their interconnects was dominated by EOF, which makes them applicable for injection of small amounts of analyte solution from one microchannel into another.[16] Our interconnects can be used as switchable ionic gates with three stable transfer levels, corresponding with a cation-pumping mode, an anion-pumping mode, and a closed-gate mode.

Figure 3b shows the ionic fluxes of Fl^{2-} (ion charge –2) and MV^{2+} (ion charge +2) through an MCM-48 interconnect versus applied potential difference. The permeability P_i of an interconnect towards a species i can be defined by $j_i = P_i \cdot \Delta c_i / L$, where j_i is the flux, Δc_i the ion concentration difference over the interconnect, and L the effective membrane thickness. Permeabilities of Fl^{2-}, MV^{2+}, and d-Trp are listed in Table 1. It is noted that for MCM-48 and γ-alumina the permeability of MV^{2+} at $\Delta V = -2$ V was much higher than the permeability of Fl^{2-} at $\Delta V = +2$ V. This can be explained by considering the combination of surface charge on the internal pore walls and the occurrence of double layer overlap in the membrane pores. The thickness of the diffuse double layer can be estimated from the Debye screening length κ^{-1}.[16] For the experiments described here, κ^{-1} is approximately 3–4 nm. Since the membrane pore sizes of the oxide films are in the range 0.8–8 nm, the double layer spans the width of the pores entirely in all cases. And since the pore surfaces of silica and γ-alumina at pH 7–8 are effectively negatively charged,[18,19] the diffuse double layer will consist mainly of positively charged ions. Hence, a higher ionic permeability is expected for cations, as indeed is found to be the case for MCM-48. The relatively non-selective behavior of the titania interconnect is related to the micropore structure of the film, i.e., the concept of a diffuse double layer, which is essentially a continuum description, is not valid any longer on length scales < 1 nm, transport is then dominated by molecule size[20] and dielectric exclusion.[21] However, because the molecular sizes are both in the region of ~ 0.8 nm and the chemical nature of the molecules is relatively similar, the permeabilities of the two molecules will also be similar.

In summary, this report describes a new class of porous oxide interconnects with a silicon nitride support structure for application in Si-based microfluidic devices. The general applicability of the fabrication method was demonstrated by constructing γ-alumina, MCM-48 silica, and amorphous titania interconnects from water- and solvent-based sols. Ionic transport was established by an externally variable potential difference across the interconnect, which allowed either cationic, anionic, or no transport depending on the magnitude and sign of the applied potential difference. It was shown that the interconnects suppress Fick diffusion of charged and uncharged species, so that they can be utilized as ionic gates with complete external control over the transport rates of anionic and cationic species. Finally, it was shown that the intrinsic ion-permselectivity of the gate at a given pH can be tuned by a proper choice of the oxide material and pore structure.

Experimental

Preparation of Oxide Sols: i) Surfactant-templated silica sols were synthesized using the cationic surfactant cetyltrimethylammonium bromide (CTAB, Aldrich) and tetraethoxyorthosilicate (TEOS, Aldrich) derived sols as described elsewhere [22]. The required amount of TEOS was mixed with 1-propanol and stirred. TEOS was then hydrolyzed by addition of an aqueous HCl solution. 2-Butanol was added to the sol and the mixture was stirred for another 30 min. The surfactant and water solution was prepared separately and added to the TEOS sol and stirred for 60 min. ii) Polymeric titania sols were prepared using titanium tetraethoxide (Aldrich) as precursor and nitric acid (Merck, 65 % solution) as acid catalyst to promote the formation of polymeric sols. A given amount of water/nitric acid solution was dissolved in alcohol and added under vigorous stirring to a titanium alkoxide/alcohol solution. The synthesis was performed in a dry nitrogen atmosphere to avoid possible reactions of the alkoxides with water vapor from ambient air. iii) Boehmite sols were prepared by a colloidal sol–gel route, in which aluminum-tri-*sec*-butoxide (Merck) was hydrolyzed in water and subsequently peptized with HNO_3 [23]. The boehmite sol was mixed with a poly(vinyl alcohol) (PVA) solution, in a PVA/boehmite mass ratio of 2:3.

Coating and Calcination: Spin-coating was used to deposit wet sols on silicon nitride Microsieves with 500 nm or 1200 nm perforations. Spin-coating was preformed under class 1000 clean room conditions in order to minimize contamination of the membrane layers. The water-based boehmite sols were applied in two successive coatings, while one coating was applied for the alcohol-based silica and titania sols. The silica layers were dried at room temperature and heated to 450 °C in air for 2 h to calcine the film and remove residual organics. The titania layers were dried in a moisture-free alcohol vapor-saturated atmosphere and calcined at 300 °C for 3 h. The boehmite layers were dried in a climate chamber at 40 °C and 60 % relative humidity (RH) to avoid crack formation in the layer. The γ-alumina phase was formed by firing the dried layers at 600 °C in air.

Materials Characterization: X-ray diffraction (XRD) patterns were recorded using a Philips SR5056 with Cu Kα radiation. Brunauer–Emmett–Teller (BET) measurements (Micromiretics) were performed at 77 K using N_2 as the condensable gas. The permporometry technique

ADVANCED MATERIALS

is described in detail in the article of Cao et al. [14]. The pore size of microporous titania was determined by the Stokes–Einstein radius model [15] from molecular weight cut-off tests with 0.5 wt.-% poly(ethylene glycol) (PEG, $M_w = 200\ g\,mol^{-1}$) solutions at 12 bar. The thickness and quality of oxide layers was checked with HR-SEM (LEO Gemini 1550 FEG-SEM, UK). Reflectometry measurements were performed on high resolution four-circle diffractometer (PHILIPS).

Received: December 19, 2003
Final version: February 13, 2004

[1] a) D. R. Reyes, D. Iossifidis, P.-A. Ayroux, A. Manz, *Anal. Chem.* **2002**, *74*, 2623. b) P.-A. Ayroux, D. Iossifidis, D. R. Reyes, A. Manz, *Anal. Chem.* **2002**, *74*, 2637. c) F. E. Regnier, B. He, S. Lin, J. Busse, *Trends Biotechnol.* **1999**, *17*, 101. d) H. Andersson, A. van den Berg, *Sens. Actuators, B* **2003**, *92*, 315.
[2] a) J. B. Edel, R. Fortt, J. C. de Mello, A. J. de Mello, *Chem. Commun.* **2002**, 1136. b) H. Wang, H. Nakamura, M. Uehara, M. Miyazaki, H. Maeda, *Chem. Commun.* **2002**, 1462. c) E. M. Chan, R. A. Mathies, A. P. Alivisatos, *Nano Lett.* **2003**, *3*, 199. d) H. Nakamura, Y. Yamaguchi, M. Miyazaki, H. Maeda, M. Uehara, P. Mulvaney, *Chem. Commun.* **2002**, 2844.
[3] A. van den Berg, T. S. J. Lammerink, *Topics Curr. Chem.* **1997**, *194*, 21.
[4] Y. Fintschenko, A. van den Berg, *J. Chromatogr., A* **1998**, *819*, 3.
[5] a) A. M. Hollman, D. Bhattacharyya, *Langmuir* **2002**, *18*, 5946. b) M. Nishizawa, V. P. Menon, C. R. Martin, *Science* **1995**, *268*, 700. c) T.-C. Kuo, D. M. Cannon, Jr., Y. Chen, J. J. Tulock, M. A. Shannon, J. V. Sweedler, P. W. Bohn, *Anal. Chem.* **2003**, *75*, 1861. d) S. B. Lee, C. R. Martin, *Anal. Chem.* **2001**, *73*, 768. e) R. B. M. Schasfoort, S. Schlautmann, J. Hendrikse, A. van den Berg, *Science* **1999**, *286*, 942.
[6] J. C. Hulteen, C. R. Martin, *J. Mater. Chem.* **1997**, *7*, 1075.
[7] T.-C. Kuo, D. M. Cannon, Jr., M. A. Shannon, P. W. Bohn, J. V. Sweedler, *Sens. Actuators, A* **2003**, *102*, 223.
[8] C. R. Martin, M. Nishizawa, K. Jirage, M. Kang, S. B. Lee, *Adv. Mater.* **2001**, *13*, 1351.
[9] a) D.-H. Park, N. Nishiyama, Y. Egashira, K. Ueyama, *Ind. Eng. Chem. Res.* **2001**, *40*, 6105. b) N. Nishiyama, D. H. Park, A. Koide, Y. Egashira, K. Ueyama, *J. Membr. Sci.* **2001**, *182*, 235. c) Y.-S. Kim, S.-M. Yang, *Adv. Mater.* **2002**, *14*, 1078.
[10] M. Klotz, A. Ayral, C. Guizard, L. Cot, *Sep. Purif. Technol.* **2001**, *25*, 71.
[11] S. Roy Chowdhury, R. Schmuhl, K. Keizer, J. E. ten Elshof, D. H. A Blank, *J. Membr. Sci.* **2003**, *225*, 177.
[12] C. J. M. van Rijn, G. J. Veldhuis, S. Kuiper, *Nanotechnology* **1998**, *9*, 343.
[13] J. Xu, Z. Luan, H. He, W. Zhou, L. Kevan, *Chem. Mater.* **1998**, *10*, 3690.
[14] G. Z. Cao, J. Meijerink, H. W. Brinkman, A. J. Burggraaf, *J. Membr. Sci.* **1993**, *83*, 221.
[15] P. Puhlfürss, A. Voigt, R. Weber, M. Morbé, *J. Membr. Sci.* **2000**, *174*, 123.
[16] P. J. Kemery, J. K. Steehler, P. W. Bohn, *Langmuir* **1998**, *14*, 2884.
[17] T.-C. Kuo, L. A. Sloan, J. V. Sweedler, P. W. Bohn, *Langmuir* **2001**, *17*, 6298.
[18] A. J. Pierre, *Introduction to Sol-Gel Processing*, Kluwer, Dordrecht, The Netherlands **1998**, p. 62.
[19] R. Schmuhl, K. Keizer, A. van den Berg, J. E. ten Elshof, D. H. A. Blank, *J. Colloid Interface Sci.* **2004**, *273*, 331.
[20] P. M. Bungay, H. Brenner, *Int. J. Multiphase Flow* **1973**, *1*, 25.
[21] J. Lyklema, in *Fundamentals of Interface and Colloid Science*, Vol. 2, Academic Press, London **1995**, Ch. 5.
[22] I. Honma, H. S. Zhou, D. Kundu, A. Endo, *Adv. Mater.* **2000**, *12*, 1529.
[23] N. Benes, A. Nijmeijer, H. Verweij, in *Membrane Science and Technology Series*, Vol. 6 (Ed: N. K. Kanellopoulos), Elsevier, Amsterdam **2000**, p. 335–372.

Synthesis of Single-Crystalline ZnO Polyhedral Submicrometer-Sized Hollow Beads Using Laser-Assisted Growth with Ethanol Droplets as Soft Templates**

By *Zhi-Yuan Jiang*, *Zhao-Xiong Xie*,* *Xian-Hua Zhang*, *Shui-Chao Lin*, *Tao Xu*, *Shu-Yuan Xie*, *Rong-Bin Huang*, and *Lan-Sun Zheng*

Nanometer or submicrometer hollow structures have attracted increasing interest recently because of their specific structure, interesting properties that differ from their solid counterparts,[1–4] and wide applications in chemistry, biotechnology, and materials science.[5–9] The fabrication of homogeneous hollow structures is also expected to open up possibilities for various new application fields, such as catalysts, controlled delivery, lightweight materials, low-dielectric-constant materials, acoustic insulation, photonic crystals, and shape-selective adsorbents.[6–10] The general approach for preparing such materials is based on the use of various removable templates or surfactant-stabilized oil-in-water emulsion droplets.[11–17] However, rupture may occur when the sacrificial core is being removed, and the products are usually aggregations of nanoparticles. Several other methods, such as template-engaged replacement reaction,[18] gas-bubble soft-template methods,[4] surface oxidation,[19] and hydrothermal and solvothermal methods,[20–22] have been developed to fabricate various nanometer or submicrometer structures with hollow interiors, which improved the crystallinity of the products. In this communication, we propose a method for the controlled synthesis of submicrometer hollow beads by laser-assisted growth using ethanol droplets as soft templates. Single-crystalline ZnO polyhedral submicrometer hollow beads have been successfully synthesized for the first time with this soft-template method. Due to the outstanding electronic and optical properties of ZnO nanostructural systems,[23] these single-crystalline ZnO polyhedral hollow beads—a new member of the ZnO nanostructure family—should find new applications.

Figure 1 illustrates the design of the scheme for the synthesis of single-crystalline ZnO polyhedral submicrometer hollow beads using laser-assisted growth with ethanol droplets as soft templates. Firstly, a mixture of Zn clusters and ethanol

[*] Prof. Z.-X. Xie, Z.-Y. Jiang, X.-H. Zhang, S.-C. Lin, T. Xu, S.-Y. Xie, Prof. R.-B. Huang, Prof. L.-S. Zheng
State Key Laboratory for Physical Chemistry of Solid Surfaces and Department of Chemistry, Xiamen University
Xiamen 361005 (P.R. China)
E-mail: zxxie@xmu.edu.cn

[**] This work was supported by the National Natural Science Foundation of China (Grant No. 20021002, 20173046, and 20273052), the Ministry of Science and Technology of China (Grant No. 2001CB610506, 2002CCA01600), the Natural Science Foundation of Fujian Province (Grant No. E0310004) and the Fok Ying-Tung Educational Foundation.

  DOI: 10.1002/adma.200306635